

Normal incidence grating spectrometer designed for inverse photoemission studies in the range 10–30 eV

P. D. Johnson and S. L. Hulbert

Physics Department, Brookhaven National Laboratory, Upton, New York 11973

R. F. Garrett^{a)}

Materials Science Department, State University of New York at Stony Brook, Stony Brook, New York 11794

M. R. Howells^{b)}

National Synchrotron Light Source, Brookhaven National Laboratory, Upton, New York 11973

(Received 30 December 1985; accepted for publication 3 April 1986)

We describe a normal incidence grating spectrometer for use in inverse photoemission studies of surfaces. We show that by operating in a configuration where the source and image are displaced from the Rowland Circle it is possible to construct a useful spectrometer that can be attached to any existing surface science chamber. The device covers the range 10–30 eV in photon energy with a typical energy resolution of 150 meV. Capable of operating with relatively low incident currents, this instrument will be an excellent choice for spin-polarized inverse photoemission experiments.

INTRODUCTION

In the last few years inverse photoemission has rapidly emerged as an experimental technique capable of providing information about the unoccupied region of the band structure of solids.¹

Electrons incident on the sample couple into some unoccupied state above the Fermi level. They then radiatively decay to a second unoccupied level above the Fermi level in a direct k -conserving transition. Measurement of the energy of the radiated photon gives the energy separation of the initial and final states and may be used as a means of determining the unoccupied density of states. The experiment, therefore, requires some form of photon detector and to date the detectors used have fallen into two categories.

First, the most popular device has been the Geiger Müller counter, primarily because of its ease of construction. The use of such counters for inverse photoemission originated in the group of V. Dose, who established the combination of a calcium fluoride (CaF_2) window backed by iodine vapor.² Such a detector works at a photon energy of 9.7 eV with a resolution of 0.7 eV. Recently, there have been two refinements to this type of detector. One revision has been to replace the CaF_2 window by a strontium fluoride window.³ This alters the photon energy of detection from 9.7 to 9.5 eV and reduces the bandwidth from 0.7 eV to 0.4 eV. An alternative refinement has been to replace the iodine by carbon disulfide whilst retaining the CaF_2 window.⁴ Such a detector has a much narrower bandwidth, typically 0.1 eV, and its photon detection energy is 10.1 eV.

However, all of the above detectors work at fixed photon energy. The second class of detector adds the possibility of tunable photon energy detection. The simplest device in this category is the refracting monochromator which employs a LiF lens as the dispersing element.^{5,6} The design recognizes that chromatic aberration in the lens will produce

strong focusing of different wavelengths near the LiF transmission cutoff. Described in more detail elsewhere,⁵ this device offers limited tunability (8–11.5 eV) with modest energy resolution (typically 0.3–0.4 eV).

Another form of tunable photon detector is the diffraction grating spectrometer. Instruments of this type offer reasonable wavelength resolution plus wavelength multiplexing, i.e., simultaneous sensitivity over all wavelengths in the recorded range. Such devices have already been described^{7,8} and were found to work efficiently in the range of 10–30 eV with a bandwidth of the order of 150 meV at the longer wavelengths of detection.

In this paper we describe a variant on this latter category and in particular describe a grating spectrometer designed to operate specifically for inverse photoemission measurements on a typical surface science chamber.

1. DESIGN CONSIDERATIONS

The traditional approach to a problem of this kind would be via a normal incidence diffraction grating spectrometer. The technology of these devices has been extensively explored for studies of both astronomical objects and terrestrial objects which have been rendered incandescent by various means.⁹

The requirement for high efficiency in the present device restricts the choice of instrument to those where only one optical element is used. We, therefore, consider only concave grating designs, and exclude plane grating instruments which require collimating and focusing optics.

The two traditional classes of concave grating devices are those which have the grating illuminated by parallel light and those which use point to point focusing. The first system is known as the Wadsworth mounting and has been modified in various ways¹⁰; the second class generally relies on the

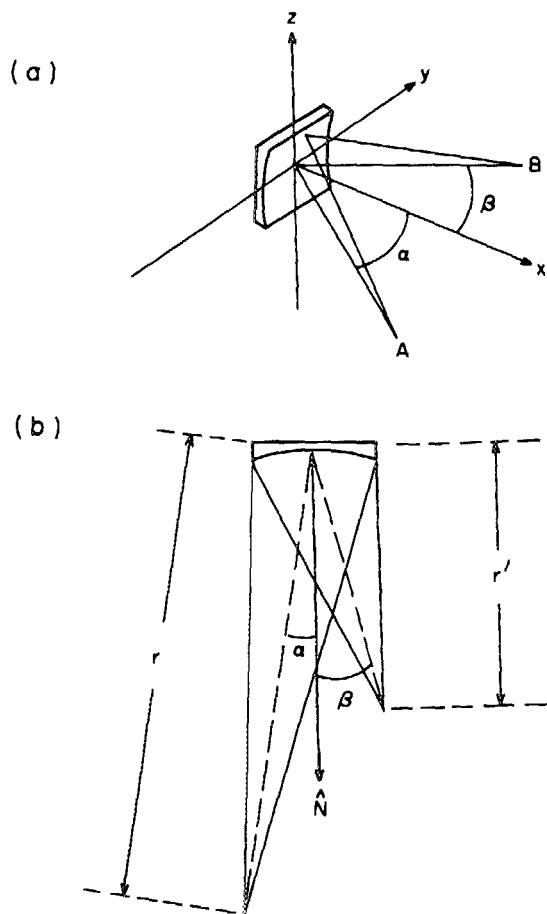


FIG. 1. Schematic diagrams of the spherical grating configuration showing (a) the coordinate system and (b) the parameters involved in the equations describing the optical system.

properties of the Rowland circle. To see how these different solutions arise we consider the optical path function F of the concave grating with groove spacing d :

$$F = r + r' + (\sin \alpha + \sin \beta - m\lambda/d)y + C_{20}y^2 + C_{02}z^2 + \text{higher-order terms.} \quad (1)$$

The notation is shown in Fig. 1, from which we see that r and α refer to the entrance arm length and the angle of incidence, respectively; r' and β are the exit arm length and the exit angle, respectively; and $C_{20}y^2$ and $C_{02}z^2$ are terms relating to defocus in the exit plane and astigmatism. The condition for the object at A to have a stigmatic focus at B is given by Fermat's principle as

$$\frac{\partial F}{\partial y} = 0, \quad \frac{\partial F}{\partial z} = 0. \quad (2)$$

Equation (1) expresses the paraxial approximation (neglect of aberrations) and shows that for focus it is necessary to satisfy both the grating equation

$$\sin \alpha + \sin \beta = m\lambda/d \quad (3)$$

and the conditions $C_{20} = C_{02} = 0$. In practice it is impossible to satisfy both of the latter conditions ($C_{20} = 0$ and $C_{02} = 0$) at the same time with a spherical grating. We thus

accept that focusing in the plane perpendicular to the symmetry plane of Fig. 1 will always be imperfect. However, this limitation does not prevent us from arriving at a useful design.

C_{20} is defined by the equation

$$2C_{20} = \left(\frac{\cos^2 \alpha}{r} - \frac{\cos \alpha}{R} \right) + \left(\frac{\cos^2 \beta}{r'} - \frac{\cos \beta}{R} \right) \equiv T + T' = 0, \quad (4)$$

where R is the radius of the spherical grating. The Wadsworth mounting satisfies this equation by choosing

$$r = \infty, \quad r' = \frac{R \cos^2 \beta}{\cos \alpha + \cos \beta}. \quad (5)$$

Whilst this represents one solution, the fact that the mounting requires the source at infinity prevents its use in the present application.

The alternative Rowland Circle condition works by setting $T = 0$ and $T' = 0$ separately, giving

$$r = R \cos \alpha, \quad r' = R \cos \beta. \quad (6)$$

Thus the object point and the image define a circle of diameter R . As stated earlier this mounting has already been shown to be a suitable basis for the design of an inverse photoemission spectrometer.⁸ However, the fact that the detector position is inconveniently close to the sample position means that the inverse photoemission experiment requires a sample chamber that is separated from any preparation area.

This situation is eased if we design a mounting where the "entrance slit" (the sample) is further from the grating than the focal plane.

Consider the possibility of satisfying Eq. (4) with $r \approx 5/3r'$. Then for a mirror ($\alpha = \beta$) the arm lengths would be $r = 4/3R \cos \alpha$ and $r' = 4/5R \cos \alpha$. Operating near normal incidence ($\cos \alpha \approx 1$), we choose $r = 4/3R$ and can compute r' from Eq. (4) using the expression

$$r' = (-T + \cos \beta/R)^{-1} \cos^2 \beta. \quad (7)$$

The dispersion in the focal plane will be given by

$$\Delta\lambda/\lambda = [\cos \beta/r'm(1/d)] \times 10^4 \text{ \AA/mm}, \quad (8)$$

where l is the coordinate in the focal plane, r' is in meters, and $1/d$ is in mm^{-1} . The magnification of the system is given by

$$M = r' \cos \alpha / r \cos \beta. \quad (9)$$

Given an electron spot beam size s on the sample we can compute the spot-size-limited resolution $\Delta\lambda$ from Eq. (8) with $\Delta l = Ms$.

Using the exit arm length r' defined by Eq. (7) and exit angle β defined by Eq. (3) we plot in Fig. 2 the focal curve for an angle of incidence of 5° and an entrance arm length of 975 mm. It will be seen from the figure that the locus of focal points for different wavelengths may be approximated by a straight line and that this allows the use of any detector of the flat field variety. The fact that the focal plane is not perfectly flat does not prove to be a limitation, as the defocused image on the flat detector is still smaller than the demagnified image of the source.

The same argument also applies to the various higher order grating aberrations. They all contribute negligible im-

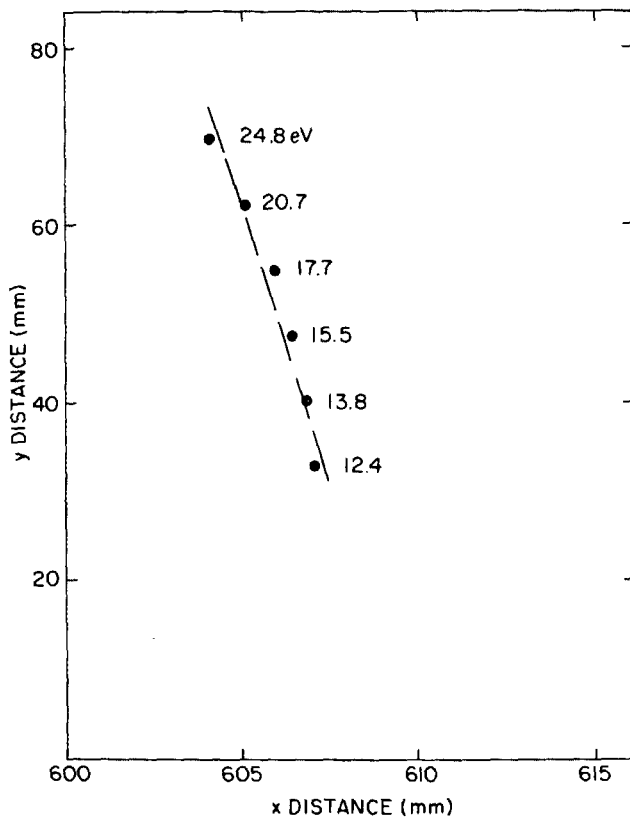


FIG. 2. Focal points at a number of different photon energies for an angle of incidence $\alpha = 5^\circ$ plotted on a coordinate system aligned with the principal incident ray (the central axis of the spectrometer chamber). The dashed line indicates the position of the flat field detector.

age broadening compared to the width of the image of the "entrance slit." The only aberration that we need to consider is astigmatism, which is the tendency for the image of an object point to become extended into a line perpendicular to the plane of incidence. This is not a disadvantage in the present design as the data-acquisition system effectively integrates along such a line. Similar reasoning also leads to the conclusion that the use of an aberration reduced holographic grating would not give any advantages to balance its disadvantage in efficiency compared to a blazed grating.

We have further recognized that, because the detection system integrates the signal perpendicular to the focal plane, it should be possible to extend the source in a direction parallel to the diffraction grooves with no loss of resolution. We have examined the possibility of using such an extended source and show ray-tracing results in Fig. 3, where we compare the image at the detector for three different photon energies emitted from a 1×1 -mm source and a 3×1 -mm source. We see from the figure that the 3×1 -mm photon source allows virtually the same resolution to be achieved in the spectrometer, but now provides the possibility of increased electron flux onto the sample with concomitant improvement in signal to noise.

II. EXPERIMENTAL APPARATUS

In this section we present details of our experimental apparatus based on the design considerations discussed in

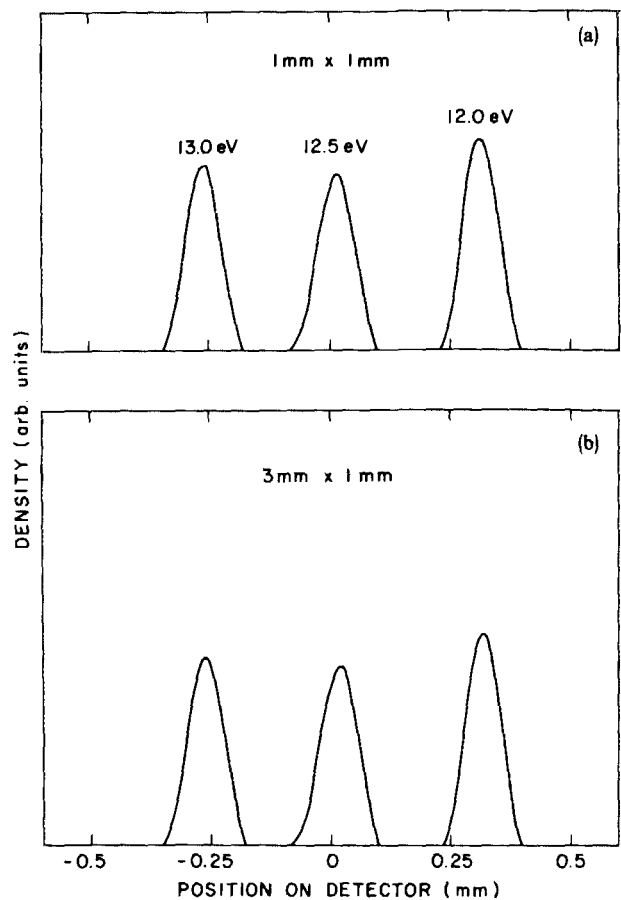


FIG. 3. Ray tracings of the images for three different photon energies emitted from (a) 1×1 -mm source and (b) 3×1 -mm source.

the previous section.

Figure 4 shows a schematic of the apparatus. The electron source has been described in detail elsewhere.¹¹ It typically provides electron currents of the order of 5 – $10 \mu\text{A}$ into a spot 1 mm in diameter with an included angle of 5° . The photons emitted from the surface are collected by a holographically ruled diffraction grating 200×150 mm.¹² This grating, which is blazed at 1000 \AA with a ruling density of 1200 lines/mm, collects approximately 0.1 sr of the emitted photon flux. The diffracted light is then focused onto a commercially available double Chevron channel plate backed by a resistive anode encoder.¹³ The front surface of the chevron, which has a width of 40 mm, is coated with CsI to improve photon detection efficiency in the energy range of interest. For the present application it is possible to use a one-dimensional detector as the signals are integrated perpendicular to the plane of incidence.

Signals from the two ends of the encoder pass through preamplifiers to a configuration of NIM modules which produce a ratio or position signal subsequently analyzed by a Le Croy Data acquisition system, operating as a PHA. The spatial resolution of the encoder is approximately 0.4 mm which corresponds to a typical wavelength resolution of the order of 5.0 \AA in the present application. Steps were taken to prevent both ions and stray ultraviolet light from entering the spectrometer chamber in order to minimize the background

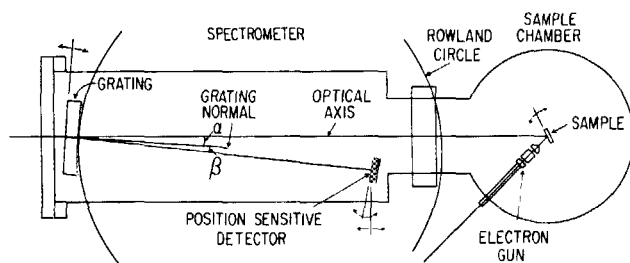


FIG. 4. Schematic of the apparatus showing the orientation of the sample, electron source, spherical grating, and position-sensitive detector.

count rate and maintain spatial uniformity across the detector.

Linearity of the detector is checked by sweeping the specularly reflected beam from the diffraction grating across the front surface of the chevron. Deviations of the order of 2% were found and corrected for near the ends of the encoder. Photon detection efficiency as a function of energy was measured by monitoring the bremsstrahlung signal from the sample resulting from higher energy electron beams (40–80 eV). These were averaged for a number of different conditions to remove any crystallographic or band structure effects. Measured efficiency curves were then used to normalize the data.

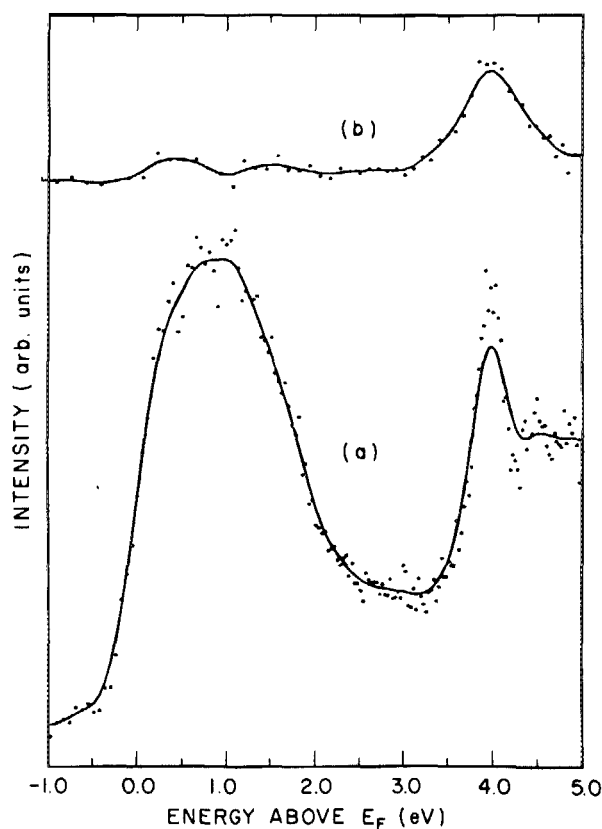


FIG. 5. Inverse photoemission spectra from a Cu(001) surface. (a) Electron beam energy 16.85 eV above the Fermi energy and beam incident along the surface normal. (b) 24.4-eV electron beam incident at 30° to the surface normal. The nearly flat background from the microchannel-plate amplifier is approximately 10–20 cts/s for the entire spectrum, which is roughly 10% of the typical signal rate.

III. DISCUSSION

In this section we present some results demonstrating the usefulness of the device. In Fig. 5 we show two inverse photoemission spectra recorded for 1 h with the electron beam incident (a) on a Cu(001) surface along the surface normal and (b) at an angle of 40° to the surface normal at the \bar{X} point in the surface Brillouin zone. The electron beam characteristics in the two cases were incident beam energy 16.85 and 24.0 eV, respectively, and incident beam currents approximately $5 \mu\text{A}$. For such currents typical count rates are of the order of 80 cts/s. The contents of these spectra have been described in more detail elsewhere.^{14,15} For the present purpose we note that the peak just below the vacuum level in Fig. 5(a), an image state, provides an excellent indication of the resolution of the system. Image states are known to have a very narrow line width, and it will be seen in Fig. 5 that the present measurement has a FWHM of 300 meV. The electron source has an energy spread of approximately 270 meV produced by the thermal spread from the 800 °C cathode, and thus we have an indication that at this photon energy ($h\nu \approx 13$ eV) the detector resolution is of the order of 130 meV. This would agree with our analysis in Sec. I for an entrance slit or electron beam spot size of 1 mm. Recently, we have measured a FWHM of 0.12 eV for the Lyman α emission line (10.2 eV) of hydrogen adsorbed on Ni(100) with this spectrometer.

The spectrum in Fig. 5(b) demonstrates the ability of the present system to record spectra with reasonable momentum resolution at high angles of incidence. The peak below the vacuum level in this spectrum is a surface state and we note that its FWHM is 0.8 eV.

In summary we have demonstrated that by operating off the Rowland circle it is possible to construct a grating spectrometer for inverse photoemission studies that may be attached to any surface science chamber. This spectrometer allows tunable photon detection over a wide range with good energy resolution. Further, we note that we have operated the device in our studies with low incident beam currents. This makes the device useful for adsorption studies, where high incident currents are not desired, and also spin-polarized inverse photoemission¹⁶ studies where the electron sources do not typically produce large currents.

ACKNOWLEDGMENTS

We would like to acknowledge useful discussions with N. V. Smith and G. C. Smith, and the expert technical assistance of F. Loeb, R. Raynis, and A. Roebuck.

This work was supported by Division of Materials Sciences U. S. Department of Energy under contract DE-ACO2-76CH00016.

^{a)} Present address: National Synchrotron Light Source, Brookhaven National Laboratory, Upton, New York 11973.

^{b)} Present address: Lawrence Berkeley Laboratory, Berkeley, CA 94720.

¹V. Dose, Prog. Surf. Sci. **13**, 225 (1983); N. V. Smith, Vacuum **33**, 803 (1983).

²G. Denninger, V. Dose, and H. Scheidt, Appl. Phys. **18**, 375 (1979).

- ³A. Goldman, M. Donath, W. Altmann, and V. Dose, *Phys. Rev.* **32**, 837 (1985).
- ⁴P. M. G. Allen, P. J. Dobson, and R. G. Egdell, *Solid State Commun.* **55**, 701 (1985).
- ⁵T. T. Childs, W. A. Royer, and N. V. Smith, *Rev. Sci. Instrum.* **55**, 1613 (1984).
- ⁶S. L. Hulbert, P. D. Johnson, N. G. Stoffel, W. A. Royer, and N. V. Smith, *Phys. Rev. B* **31**, 6815 (1985).
- ⁷Th. Fauster, F. J. Himpsel, J. J. Donelon, and A. Marx, *Rev. Sci. Instrum.* **54**, 68 (1983).
- ⁸Th. Fauster, D. Straub, J. J. Donelon, D. Grimm, A. Marx, and F. J. Himpsel, *Rev. Sci. Instrum.* **56**, 1212 (1985).
- ⁹e.g., J. A. R. Samson, *Techniques of Vacuum Ultraviolet Spectroscopy* (Pied, Lincoln, NE, 1967).
- ¹⁰e.g., M. R. Howells, *Nucl. Instrum. Methods* **195**, 215 (1982).
- ¹¹N. G. Stoffel and P. D. Johnson, *Nucl. Instrum. Methods A* **234**, 230 (1985).
- ¹²Jobin-Yvon Instruments SA Inc., 173 Essex Avenue, Metuchen, NJ 08840.
- ¹³Surface Science Laboratories, Inc., 1206 Charleston Rd., Mountain View, CA 94043.
- ¹⁴S. L. Hulbert, P. D. Johnson, M. Weinert, and R. F. Garrett, *Phys. Rev. B* **33**, 760 (1986).
- ¹⁵S. L. Hulbert, P. D. Johnson, and R. F. Garrett (to be published).
- ¹⁶e.g., J. Unguris, A. Seiler, R. J. Celotta, D. T. Pierce, P. D. Johnson, and N. V. Smith, *Phys. Rev. Lett.* **49**, 1047 (1982).